

# Recurrent Events Modeling Based on a Reflected Brownian Motion with Application to Hypoglycemia

Yingfa Xie<sup>1</sup>, Haoda Fu<sup>2</sup>, Yuan Huang<sup>3</sup>, Vladimir Pozdnyakov<sup>1</sup> and Jun Yan <sup>\*1</sup>

<sup>1</sup>*Department of Statistics, University of Connecticut*

<sup>2</sup>*Eli Lilly and Company*

<sup>3</sup>*Department of Biostatistics, Yale School of Public Health*

## Abstract

Patients with type 2 diabetes need to closely monitor blood sugar levels as their routine diabetes self-management. Although many treatment agents aim to tightly control blood sugar, hypoglycemia often stands as an adverse event. In practice, patients can observe hypoglycemic events more easily than hyperglycemic events due to the perception of neurogenic symptoms. We propose to model each patient's observed hypoglycemic event as a lower-boundary crossing event for a reflected Brownian motion with an upper reflection barrier. The lower-boundary is set by clinical standards. To capture patient heterogeneity and within-patient dependence, covariates and a patient level frailty are incorporated into the volatility and the upper reflection barrier. This framework provides quantification for the underlying glucose level variability, patients heterogeneity, and risk factors' impact on glucose. We make inferences based on a Bayesian framework using Markov chain Monte Carlo. Two model comparison criteria, the Deviance Information Criterion and the Logarithm of the Pseudo-Marginal Likelihood, are used for model selection. The methodology is validated in simulation studies. In analyzing a dataset from the diabetic patients in the DURABLE trial, our model provides adequate fit, generates data similar to the observed data, and offers insights that could be missed by other models.

*Keywords:* first hitting time; frailty; MCMC; recurrent event; threshold regression

---

\*Email address: jun.yan@uconn.edu; corresponding author

# 1 Introduction

Diabetes is a group of disease characterized by elevated blood glucose. It is a major cause of kidney failure, non-traumatic lower-limb amputations, blindness, heart disease, and stroke. As a result, diabetes is one of the leading causes of death. Diabetes affects 37.3 million Americans which is 11.3% of the US population ([Centers for Disease Control and Prevention, 2022](#)). The goal of treating diabetes patients is to lower their blood glucose in range. When blood glucose level is too high, patients will experience *hyperglycemia*. Lowering glucose too much, however, could result in an adverse event called *hypoglycemia*. Concern over hypoglycemia has a significant negative impact on diabetes management, making it a major factor to prevent patients' glycemic control from reaching treatment target ([Wild et al., 2007](#)). It is desired to develop new anti-diabetes agents that lead to less hypoglycemic events while lowering the glucose toward the normal range.

Hypoglycemias are relatively easier observed than hyperglycemias in practice. Symptoms of hypoglycemia are the result of brain glucose deprivation or the perception of physiological change. Awareness of hypoglycemia is mainly the result of the perception of neurogenic symptoms ([Towler et al., 1993](#); [DeRosa and Cryer, 2004](#)). Times of hypoglycemic events are recorded through patients' self-report diaries with easily observed symptoms, such as headache, shaking, sweating, hunger, and fast heartbeat ([Cryer et al., 2003](#)). In contrast, hyperglycemia symptoms are much less obvious, and may not be noticed unless a blood sugar level test is performed ([Cryer et al., 2009](#)). Therefore, only the times of recurrent hypoglycemic events are reliably available in self-reported data. These event times have been the target of modeling in diabetes clinical research (e.g., [Fu et al., 2016](#); [Ma et al., 2021](#); [Doubleday et al., 2022](#)).

A variety of recurrent event models have been available. Earlier works characterize the intensity function of the recurrent event process ([Andersen and Gill, 1982](#)). The multiple events can be analyzed with the conditional intensity for the sequence of events given the history ([Prentice et al., 1981](#); [Lee et al., 1992](#)) or with marginal intensities of the gaps

between successive events (Wei et al., 1989; Huang and Chen, 2003; Schaubel and Cai, 2004). Alternative approaches to gap times have been proposed, such as accelerated failure time model (Chang, 2004), additive hazards model (Sun et al., 2006), and quantile regression (Luo et al., 2013). Heterogeneities beyond covariates can be incorporated in the models as a subject-level random effect which also captures the dependency between events within an individual (Klein, 1992; Duchateau et al., 2003; Box-Steffensmeier and De Boef, 2006). Less restrictive model assumptions have been considered by marginal rate or marginal mean models (Lawless and Nadeau, 1995; Lin et al., 2000), which do not fully specify the recurrent event process. More recently, a general scale-change model encompasses multiple existing event time models in a unified framework and allows a flexible form of informative censoring (Xu et al., 2020). The readers are referred to recent reviews for details (Cook and Lawless, 2007; Charles-Nelson et al., 2019).

An alternative approach is the first hitting time (FHT) model. An FHT model has three components: a stochastic process, a boundary, and a time scale on which the process unfolds (Lee, 2019). An event occurs when the underlying stochastic process hits the preset boundary. It is well-known that the distribution of the FHT of a Brownian motion is the inverse Gaussian distribution (Schrödinger, 1915; Folks and Chhikara, 1978). Incorporating covariates into the model parameters leads to threshold regression (Lee and Whitmore, 2006). Random effects can be incorporated to account for unmeasured covariates (Pennell et al., 2010). For recurrent events, Whitmore et al. (2012) modeled the event times as a sequence of independent and identically distributed hitting times of a Wiener process as it passes through successive equally-spaced levels. Economou et al. (2015) extended the inverse Gaussian threshold regression model with a random effect. Malefaki et al. (2015) further extended the model to allow censoring to occur at every intermediate stage during the recurrent event process. For recurrent hypoglycemic events of diabetic patients, it is natural to model them as hitting times when the glucose level crosses a lower barrier but the unobserved hyperglycemic event times need to be handled.

We propose to model hypoglycemic event times as the FHTs of a Brownian motion with an upper reflection boundary hitting a lower barrier. The upper reflection barrier represents that patients' glucose levels will eventually decrease, potentially due to the use of glucose-lowering medications that are routinely prescribed for this patient population. Consequently, hyperglycemic events at which the patient's glucose levels hit the upper reflection barrier are typically not observed. Conversely, the lower barrier represents a boundary beyond which patients experience uncomfortable symptoms associated with hypoglycemia. As a result, hitting times for the lower barrier are typically observed. The distribution of the FHT of the lower barrier of a Brownian motion with an upper reflection barrier has been studied by [Hu et al. \(2012\)](#). Taking advantage of this distribution, we model the recurrent hypoglycemic events based on a sequence of reflected Brownian motions hitting a lower barrier, after which the process restarts at a preset point between the two barriers. The gap times between the successive events of the same patient are assumed to be independent conditional on a subject-level random effect. Covariates and a subject-level random effect are linked to parameters of the FHT model. The model provides unique opportunities to characterize the variability and heterogeneity of hypoglycemic events with an intuitive interpretation.

Replacing the Brownian motion with a reflected Brownian motion in an FHT model introduces a significant level of complexity. The density and the distribution functions of the FHT derived in [Hu et al. \(2012\)](#) have not been used in the statistical literature. Both functions involve infinite series, which present challenges to accurate evaluation of the log-likelihood and efficient design of random number generation. To address the challenges, we first demonstrated that the right tail of the FHT is bounded by an exponential rate. Drawing on this result, we implemented the density and distribution functions and formulated an efficient rejection sampling algorithm with a three-piece proposal density. Inferences are conducted within a Bayesian framework using Markov chain Monte Carlo (MCMC) with our implementation of the FHT distribution incorporated into the generic algorithm in R package NIMBLE ([de Valpine et al., 2017](#)). Different models, especially those with

different types of random effects, are compared with two Bayesian model comparison criteria, deviance information criterion (DIC) (Spiegelhalter et al., 2002) and logarithm of the pseudo-marginal likelihood (LPML) (Geisser and Eddy, 1979; Gelfand and Dey, 1994). The whole methodology was validated in numerical studies before being applied to analyze the hypoglycemic event data in our motivating application. The R code is publicly available in <https://github.com/YingfaX/reflbrown>.

The remainder of the article is organized as follows. In Section 2, an FHT model of a reflected Brownian motion is set up and an efficient rejection sampling algorithm is proposed for simulation from the model. Bayesian parameter estimation and model selection methods are presented in Section 3. Simulation studies that validate the Bayesian inferences are reported in Section 4. The methodologies are applied to the hypoglycemic event times from the DURABLE trial (ClinicalTrials.gov Identifier: NCT00279201) in Section 5. Section 6 concludes with a discussion.

## 2 Model

The fundamental component of our model is the FHT model for the first time when a Brownian motion with a reflecting upper barrier hits a lower barrier. A sequence of such models are assembled for recurrent events. Subsequently, we incorporate covariates and frailty terms in the model parameters to further characterize variability and heterogeneity.

### 2.1 FHT of a reflected Brownian motion

Consider a no-drift Brownian motion  $X(t)$  with volatility  $\sigma$ . Without loss of generality, let  $\kappa$  be the upper reflection barrier  $\kappa > 0$  and  $\nu = 0$  be the lower barrier. Suppose that  $X(0) = x_0 \in [0, \kappa]$  is the starting point. The first time when  $X(t)$  hits  $\nu$  is  $\tau := \inf\{t > 0; X(t) = \nu\}$ . For any  $\nu \in [0, x_0)$ , the density and distribution function of  $\tau$  are, respectively (Hu et al.,

2012),

$$f(t|x_0, \nu, \kappa, \sigma) = \sum_{n=1}^{\infty} c_n \lambda_n e^{-\lambda_n t}, \quad t > 0, \quad (2.1)$$

$$F(t|x_0, \nu, \kappa, \sigma) = 1 - \sum_{n=1}^{\infty} c_n e^{-\lambda_n t}, \quad t > 0, \quad (2.2)$$

where for  $n = 1, 2, \dots$ ,

$$\lambda_n = \frac{(2n-1)^2 \sigma^2 \pi^2}{8(\kappa - \nu)^2}, \text{ and } c_n = \frac{(-1)^{n+1} 4}{(2n-1)\pi} \cos\left(\frac{(2n-1)\pi(\kappa - x_0)}{2(\kappa - \nu)}\right).$$

Note that  $0 < \lambda_1 < \lambda_2 < \dots$ ,  $\lambda_n \rightarrow \infty$ , and  $\sum_{n=1}^{\infty} c_n = 1$ . It is tempting to think of  $f(t)$  as a mixture of exponential densities, but this is not true because  $c_n$ 's can be negative.

Random number generation from density (2.1) has not been investigated in the literature, we propose a rejection sampling algorithm. By construction, the proposal density  $g(t)$  is required such that  $f(t)/g(t)$  is bounded over the support  $t > 0$ . It is known that  $f(t)/t \rightarrow 0$  as  $t \downarrow 0$  (Hu et al., 2012, p. 13). In Appendix A, we show that the right tail of  $f(t)$  is bounded by that of an exponential density with rate  $\lambda_1$ :

$$f(t) \sim c_1 \lambda_1 \exp(-\lambda_1 t) \text{ as } t \rightarrow \infty.$$

Given these properties, we propose a three-piece proposal density which consists a left tail, a body, and a right tail. The left tail is a triangular density that connects the origin to the peak of the target density peak  $(t_m, f(t_m))$ , where  $t_m$  is the mode of the target density  $f$ . The body is a trapezoid density that connects the peak  $(t_m, f(t_m))$  to a user-defined  $q^{th}$  quantile point  $(t_q, f(t_q))$  where  $t_q$  is the upper  $q$ th quantile of  $f$ , and  $q$ , for example, can be set to be 0.95. The right tail beyond  $t_q$  is the tail of the exponential density with rate  $\lambda_1$ . The details of the implementation of the algorithm is in Appendix B.

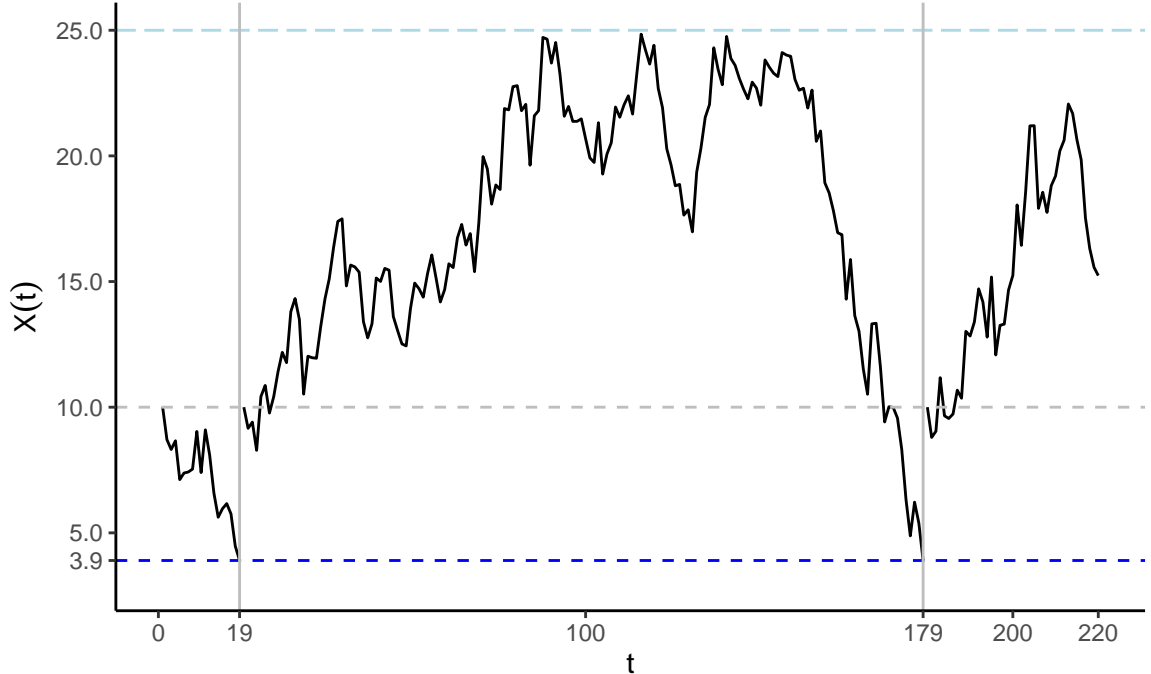


Figure 1: A sample path (black solid line) of the reflected Brownian motion with  $x_0 = 10$  (grey dash line),  $\kappa = 25$  (lightblue dash line),  $\nu = 3.9$  (blue dash line), and  $\sigma = 3$ . Two events occur at time  $T_1 = 19$  and  $T_2 = 179$ , respectively, as marked by the gray vertical lines. Observation is censored at time 220.

## 2.2 Modeling gap times of hypoglycemic events

We model the recurrent hypoglycemic events based on a sequence of reflected Brownian motions hitting a lower barrier  $\nu$ . The Brownian motion has volatility  $\sigma$  and an unobserved reflection upper barrier  $\kappa$ , beyond which hyperglycemia occurs but may not be recorded. The reflected Brownian motion restarts at a known starting point  $x_0$  after hitting the lower barrier  $\nu$ , where  $x_0$  can be set as the average level from the patients group. This is motivated by that patients' glucose level arises back, possibly after eating to relieve quickly the symptoms of hypoglycemia. The gap times between two successive hypoglycemic events thus follow a FHT distribution. Figure 1 shows a sample path for a subject who experiences two events at time  $T_1 = 19$  and  $T_2 = 179$ , and finally is censored at time 220.

To incorporate heterogeneity, we allow volatility  $\sigma$  and upper barrier  $\kappa$  to depend on subject-level covariates. Appropriate link functions are necessary to ensure that  $\sigma > 0$  and

$\kappa > x_0$ . Subject-level random effects can be further added to the regression. In particular, the models for  $\sigma_i$  and  $\kappa_i$  with the log link are

$$\log(\sigma_i) = \mathbf{X}_i^\top \boldsymbol{\beta} + Z_{i1}, \quad \text{and} \quad \log(\kappa_i - x_0) = \mathbf{X}_i^\top \boldsymbol{\alpha} + Z_{i2},$$

respectively, where  $\mathbf{X}_i$  is a  $p$ -dimensional covariate vector for subject  $i$ ,  $\boldsymbol{\beta}$  and  $\boldsymbol{\alpha}$  are  $p$ -dimensional regression coefficient vectors, and  $(Z_{i1}, Z_{i2})$  is a bivariate normal random effect with mean  $\mathbf{0}$ , variance  $\boldsymbol{\theta} = (\theta_1, \theta_2)$ , and correlation  $\rho$ . Also note that,  $\mathbf{X}_i$  is considered as time-independent covariate vector.

For ease of implementation, the bivariate normal vector  $(Z_{i1}, Z_{i2})$  can be reparametrized as  $(Z_{i1}, \gamma Z_{i1} + Z'_{i2})$ , where  $Z_{i1}$  and  $Z'_{i2}$  are independent normal variables with mean zero and variance  $\theta_1$  and  $\theta'_2$ , respectively. Then the variance of  $Z_{i2}$ ,  $\theta_2$ , is reparametrized as  $\gamma^2 \theta_1 + \theta'_2$ , and the correlation  $\rho$  between  $Z_{i1}$  and  $Z_{i2}$  is reparametrized as  $\gamma \sqrt{\theta_1 / (\gamma^2 \theta_1 + \theta'_2)}$ . The reparametrized models for  $\sigma_i$  and  $\kappa_i$  are, respectively,

$$\log(\sigma_i) = \mathbf{X}_i^\top \boldsymbol{\beta} + Z_{i1}, \quad \text{and} \quad \log(\kappa_i - x_0) = \mathbf{X}_i^\top \boldsymbol{\alpha} + \gamma Z_{i1} + Z'_{i2}. \quad (2.3)$$

The starting point  $x_0$  and lower barrier  $\nu$  are set to be fixed depending on the real data and clinical trial standard, which are shared for all subjects. In general, the subject with higher volatility and smaller reflected barrier is associated with higher risk of hypoglycemic event.

### 3 Bayesian Inference

Suppose that the event times of hypoglycemia are observed for a group of  $n$  patients during their follow-up times. For  $i = 1, \dots, n$ , let  $t_{ij}$ ,  $j = 1, \dots, n_i$  be the  $j$ th of the  $n_i$  observed gap times of subject  $i$ , the last of which is usually censored; let  $\delta_{ij} = 1$  if  $t_{ij}$  is an event and 0 otherwise. In addition to a  $p$ -dimensional covariate vector  $\mathbf{X}_i$ , the observed data include  $\mathbf{t}_i = (t_{i1}, \dots, t_{in_i})^\top$  and  $\boldsymbol{\delta}_i = (\delta_{i1}, \dots, \delta_{in_i})^\top$ ,  $i = 1, \dots, n$ . The parameters to be estimated



are  $\boldsymbol{\Omega} = (\boldsymbol{\alpha}^\top, \boldsymbol{\beta}^\top, \theta_1, \theta'_2, \gamma)^\top$ .

### 3.1 Likelihood, prior, and posterior

Given the covariate vector  $\mathbf{X}_i$  and subject-level frailties  $\mathbf{z}_i = (z_{i1}, z'_{i2})$ , the gap times of subject  $i$  are assumed to be conditionally independent. The conditional likelihood contribution of subject  $i$  given the unobserved frailties is

$$L_i(\boldsymbol{\Omega} | \mathbf{t}_i, \boldsymbol{\delta}_i, \mathbf{X}_i, \mathbf{z}_i) = \prod_{j=1}^{n_i} [f(t_{ij} | x_0, \nu, \kappa_i, \sigma_i)]^{\delta_{ij}} [1 - F(t_{ij} | x_0, \nu, \kappa_i, \sigma_i)]^{(1-\delta_{ij})},$$

where the density and distribution functions are given by (2.1) and (2.2), respectively, and  $\sigma_i$  and  $\kappa_i$  are defined in (2.3).

In practice, the recorded event times are usually discrete in the unit of days. This can be accounted for by assuming that the  $t_{ij}$ 's are interval-censored. The contribution to the likelihood of subject  $i$  is then rewritten as

$$L_i(\boldsymbol{\Omega} | \mathbf{t}_i, \boldsymbol{\delta}_i, \mathbf{X}_i, \mathbf{z}_i) = \prod_{j=1}^{n_i} [F^*(t_{ij} | x_0, \nu, \kappa_i, \sigma_i)]^{\delta_{ij}} \left[ 1 - F\left(t_{ij} + \frac{1}{2} \middle| x_0, \nu, \kappa_i, \sigma_i\right) \right]^{(1-\delta_{ij})}, \quad (3.1)$$

where

$$F^*(t_{ij} | x_0, \nu, \kappa_i, \sigma_i) = F\left(t_{ij} + \frac{1}{2} \middle| x_0, \nu, \kappa_i, \sigma_i\right) - F\left(t_{ij} - \frac{1}{2} \middle| x_0, \nu, \kappa_i, \sigma_i\right).$$

Prior distributions of the parameters need to be specified to complete the Bayesian model. For regression coefficients  $\boldsymbol{\alpha}$  and  $\boldsymbol{\beta}$ , normal priors with zero mean and a large variance are specified. Inverse gamma priors are specified for the normal variances of the frailties  $\theta_1$  and  $\theta'_2$ . For the reparametrized coefficient of the frailty  $\gamma$ , a vague normal prior with mean zero is imposed. The priors are summarized as follows:

$$\alpha_l \sim N(0, \sigma_\alpha^2), \quad l = 1, \dots, p,$$

$$\begin{aligned}
\beta_l &\sim N(0, \sigma_\beta^2), \quad l = 1, \dots, p, \\
\gamma &\sim N(0, \sigma_\gamma^2), \\
\theta_1 &\sim \text{IG}(a, b), \\
\theta'_2 &\sim \text{IG}(a, b),
\end{aligned} \tag{3.2}$$

where  $N(0, \nu^2)$  is the normal distribution with mean zero and variance  $\nu^2 > 0$ , and  $\text{IG}(a, b)$  is the inverse gamma distribution with shape  $a > 0$  and scale  $b > 0$ . In our numerical studies, the hyper-parameters were set to be  $\sigma_\alpha^2 = \sigma_\beta^2 = \sigma_\gamma^2 = 10^2$ , and  $a = b = 1$ .

With  $\mathbf{z} = (\mathbf{z}_1, \dots, \mathbf{z}_n)^\top$ , combining the likelihood function and prior distributions leads to the joint posterior density

$$\pi(\boldsymbol{\Omega}, \mathbf{z} | \mathbf{t}_i, \boldsymbol{\delta}_i, \mathbf{X}_i) \propto \left[ \prod_{i=1}^n L_i(\boldsymbol{\Omega} | \mathbf{t}_i, \boldsymbol{\delta}_i, \mathbf{X}_i, \mathbf{z}_i) g(\mathbf{z}_i | \theta_1, \theta'_2) \right] \left[ \prod_{l=1}^p q(\alpha_l) q(\beta_l) \right] q(\theta_1) q(\theta'_2) q(\gamma),$$

where  $q(\cdot)$  denotes a generic density function of its argument,  $L_i(\boldsymbol{\Omega} | \mathbf{t}_i, \boldsymbol{\delta}_i, \mathbf{X}_i, \mathbf{z}_i)$  is the conditional likelihood function for subject  $i$  given in (3.1),  $g(\mathbf{z}_i | \theta_1, \theta'_2)$  is the bivariate independent normal density of the reparametrized frailties of subject  $i$ , and all the  $q(\cdot)$ 's are priors given in (3.2). Since all the priors are proper, the posterior is proper.

To make inferences about the parameters, we use MCMC. Draws from the posterior distribution are drawn by a Gibbs sampling algorithm. The full conditional distributions of all the parameters are sampled with the Metropolis–Hasting algorithm because the FHT density is not of any existing standard form. We incorporated our customized FHT distribution into a generic implementation through R package NIMBLE (de Valpine et al., 2017). Due to the large number of unobserved frailties, the resulting chains are highly auto-correlated. A good number of draws can be obtained after thinning those long chains.

### 3.2 Model selection

With  $\text{Dev}(\boldsymbol{\Omega})$  denoting the deviance calculated by negated observed-data loglikelihood evaluated at  $\boldsymbol{\Omega}$ , DIC is given as

$$\text{DIC} = \text{Dev}(\bar{\boldsymbol{\Omega}}) + 2p_D,$$

where  $\bar{\boldsymbol{\Omega}}$  is the posterior mean of  $\boldsymbol{\Omega}$ ,  $p_D = \overline{\text{Dev}}(\boldsymbol{\Omega}) - \text{Dev}(\bar{\boldsymbol{\Omega}})$  is the effective number of parameters, and  $\overline{\text{Dev}}(\boldsymbol{\Omega})$  is the posterior mean of  $\text{Dev}(\boldsymbol{\Omega})$ . This calculation based on the observed-data likelihood is the DIC<sub>3</sub> in [Celeux et al. \(2006\)](#). Since there is no closed-form of the observed-data likelihood, we used Monte Carlo integration to approximate it. The observed-data likelihood of subject  $i$  has the form

$$L_i(\boldsymbol{\Omega}|\mathbf{t}_i, \boldsymbol{\delta}_i, \mathbf{X}_i) = \int L_i(\boldsymbol{\Omega}|\mathbf{t}_i, \boldsymbol{\delta}_i, \mathbf{X}_i, \mathbf{z}_i)g(\mathbf{z}_i|\theta_1, \theta_2)d\mathbf{z}_i,$$

where  $L_i(\boldsymbol{\Omega}|\mathbf{t}_i, \boldsymbol{\delta}_i, \mathbf{X}_i, \mathbf{z}_i)$  is given in (3.1). The Monte Carlo approximation for the observed-data likelihood for subject  $i$  is

$$L_i(\boldsymbol{\Omega}|\mathbf{t}_i, \boldsymbol{\delta}_i, \mathbf{X}_i) \approx \frac{1}{M} \sum_{m=1}^M L_i(\boldsymbol{\Omega}|\mathbf{t}_i, \boldsymbol{\delta}_i, \mathbf{X}_i, \mathbf{z}_i^{(m)}), \quad (3.3)$$

where  $\mathbf{z}_i^{(1)}, \dots, \mathbf{z}_i^{(M)}$  are Monte Carlo samples that each can be easily generated by the independent normal distributions, and  $M$  is the Monte Carlo sample size. The deviance is given by

$$\text{Dev}(\boldsymbol{\Omega}) = -2 \sum_{i=1}^n \log L_i(\boldsymbol{\Omega}|\mathbf{t}_i, \boldsymbol{\delta}_i, \mathbf{X}_i).$$

Models with smaller DIC values are preferred.

The other criterion LPML is calculated based on conditional predictive ordinate (CPO). Let  $D_{-i} = \{(\mathbf{t}_j, \boldsymbol{\delta}_j, X_j) : j = 1, \dots, n; j \neq i\}$ , denote the observed data with the  $i$ th subject

excluded. The CPO for the  $i$ th subject is the leave-one-out predictive likelihood

$$\text{CPO}_i = \int L_i(\boldsymbol{\Omega}|\mathbf{t}_i, \boldsymbol{\delta}_i, \mathbf{X}_i)q(\boldsymbol{\Omega}|D_{-i})d\boldsymbol{\Omega},$$

where  $q(\boldsymbol{\Omega}|D_{-i})$  is the marginal posterior distribution of  $\boldsymbol{\Omega}$  with the  $i$ th subject excluded.

The Monte Carlo estimate of  $\text{CPO}_i$  (Dey et al., 1997) is

$$\widehat{\text{CPO}}_i = \left[ \frac{1}{K} \sum_{k=1}^K \frac{1}{L_i(\boldsymbol{\Omega}|\mathbf{t}_i, \boldsymbol{\delta}_i, \mathbf{X}_i)} \right]^{-1}, \quad (3.4)$$

where  $\boldsymbol{\Omega}^{(k)} = (\boldsymbol{\alpha}^{(k)}, \boldsymbol{\beta}^{(k)}, \theta_1^{(k)}, \theta_2^{(k)}, \gamma^{(k)})^\top$ ,  $k = 1, \dots, K$ , is the  $k$ th iteration of posterior draws. Each term  $L_i$  in Equation (3.4) can be approximated the same way as in (3.3). Then the LPML can be calculated by

$$\widehat{\text{LPML}} = \sum_{i=1}^n \log(\widehat{\text{CPO}}_i).$$

Models with higher LPML values are preferred.

## 4 Simulation

Simulation studies were conducted to evaluate the performance of the Bayesian estimator and the model selection criteria. To mimic the real application analyzed in the next section, we considered a setting of two covariates for each subject  $i$ :  $X_{i1}$ , baseline insulin level and  $X_{i2}$ , baseline body mass index (BMI). A bivariate gamma distribution with a normal copula was fitted to the real data with R package copula (Hofert et al., 2018). The covariates were then generated from the fitted bivariate gamma distribution.

Three frailty models were used to generate recurrent events with covariate vector  $\mathbf{X}_i = (1, X_{i1}, X_{i2})^\top$ . Model 1 is the full model (2.3) with  $\boldsymbol{\alpha} = (2.9, 0.2, -0.1)^\top$ ,  $\boldsymbol{\beta} = (0.9, -0.2, -0.1)^\top$ , and  $\gamma = -0.55$ ; the frailties  $z_{i1}$  and  $z'_{i2}$  were generated from the normal distribution with

mean zero and variance  $\theta_1 = 0.2$  and  $\theta'_2 = 0.3$ , respectively. The starting point  $x_0$  and the lower barrier  $\nu$  were set to be  $x_0 = 10$  and  $\nu = 3.9$ , respectively, which will be discussed in Section 5. Model 2 is the same as Model 1 except that  $\gamma = 0$ , which means that the frailties in the upper reflection barrier and the volatility are independent. Model 3 is also a reduced model of Model 1 with the restrictions  $\gamma = -1$  and  $\theta'_2 = 0$ , which implies that the upper reflection barrier and the volatility share the same frailty. The negative sign of gamma was chosen as suggested by the real data analysis. For ease of reference, the three models are referred to as, respectively, correlated-frailty, independent-frailty, and shared-frailty.

For each model, the gap times were generated with the rejection sampling algorithm in Section 2.1 until the sum of generated gap times is equal to or larger than the follow-up time of each subject  $i$ , where the follow-up times were independently generated from the empirical distribution of the follow-up times of the real data. The generated gap times were then rounded into integers as days. Two levels of sample sizes,  $n \in \{200, 400\}$  were considered. For each simulation setting, 200 datasets were generated.

The Bayesian analysis of each dataset used prior distributions specified in Equation (3.2). For the coefficient parameters, we set  $\sigma_\alpha^2 = \sigma_\beta^2 = \sigma_\gamma^2 = 10^2$ , which leads to vague but proper prior distributions. The hyper-parameters  $(a, b)$  of the inverse gamma prior for the frailty variances are often set to be  $a = b = 1$  (Gelman, 2006; Manda and Meyer, 2005). Given a dataset, an MCMC was run with 90,000 iterations. The first 15,000 iterations were discarded as burn-in period and the rest were thinned by 150. The convergence of MCMC was checked with Heidelberger & Welch's diagnostic (Heidelberger and Welch, 1983), which is available in R package CODA (Plummer et al., 2006). The posterior inferences and model selection criteria were obtained based on the resulting 500 MCMC samples. The choice of posterior sample size, 500, was driven by the consideration to reduce computational cost for the calculation of DIC/LPML criteria. Those criteria were calculated based on observed likelihood that involves integrating over the random effect with Monte Carlo approximation, which is time-consuming. To further justify the independence of the posterior samples, the

Table 1: Results of parameter estimation under correct specifications for three models with sample size  $n \in \{200, 400\}$ . SD, posterior standard deviation; ESD, empirical standard deviation; CR, coverage rate of 95% HPD credible intervals.

Model	Para	True	$n = 200$				$n = 400$			
			Bias	SD	ESD	CR	Bias	SD	ESD	CR
correlated-frailty	$\alpha_0$	2.90	0.090	0.166	0.171	0.90	0.050	0.105	0.112	0.92
	$\alpha_1$	0.20	0.051	0.151	0.152	0.92	0.019	0.096	0.097	0.96
	$\alpha_2$	-0.10	0.004	0.111	0.104	0.96	-0.001	0.072	0.073	0.96
	$\gamma$	-0.55	0.011	0.298	0.257	0.96	-0.019	0.199	0.203	0.96
	$\beta_0$	0.90	-0.016	0.047	0.048	0.92	-0.003	0.032	0.033	0.95
	$\beta_1$	-0.20	-0.006	0.052	0.048	0.96	0.002	0.035	0.032	0.96
	$\beta_2$	-0.10	0.001	0.048	0.051	0.93	-0.001	0.033	0.033	0.95
	$\theta_1$	0.20	0.029	0.038	0.036	0.90	0.010	0.025	0.026	0.92
	$\theta'_2$	0.30	0.129	0.140	0.115	0.89	0.057	0.086	0.077	0.92
independent-frailty	$\alpha_0$	2.90	0.076	0.128	0.110	0.95	0.037	0.084	0.078	0.94
	$\alpha_1$	0.20	0.052	0.149	0.143	0.95	0.017	0.099	0.096	0.94
	$\alpha_2$	-0.10	-0.005	0.107	0.096	0.96	-0.002	0.071	0.072	0.92
	$\beta_0$	0.90	-0.010	0.047	0.045	0.96	-0.008	0.033	0.031	0.94
	$\beta_1$	-0.20	-0.009	0.053	0.050	0.93	0.000	0.036	0.038	0.96
	$\beta_2$	-0.10	0.006	0.048	0.049	0.94	-0.001	0.033	0.034	0.93
	$\theta_1$	0.20	0.029	0.037	0.033	0.92	0.015	0.025	0.023	0.92
	$\theta'_2$	0.30	0.102	0.126	0.099	0.95	0.062	0.083	0.077	0.90
	shared-frailty	$\alpha_0$	2.90	0.042	0.126	0.124	0.97	0.011	0.082	0.081
$\alpha_1$		0.20	0.022	0.104	0.105	0.93	0.005	0.069	0.072	0.94
$\alpha_2$		-0.10	-0.002	0.078	0.065	0.98	0.001	0.052	0.051	0.94
$\gamma$		-1.00	-0.038	0.202	0.188	0.98	0.011	0.134	0.143	0.93
$\beta_0$		0.90	-0.018	0.046	0.051	0.90	-0.012	0.032	0.031	0.94
$\beta_1$		-0.20	-0.008	0.050	0.053	0.92	-0.003	0.035	0.036	0.93
$\beta_2$		-0.10	-0.003	0.046	0.044	0.95	-0.004	0.032	0.032	0.92
$\theta_1$		0.20	0.025	0.036	0.034	0.90	0.013	0.024	0.020	0.96

effective sample size was calculated for the 500 MCMC samples using the R package CODA. The average effective sample size is at least 332 among parameters of different models across 200 simulation replicates, which we believe is reasonable for inferences.

Table 1 summarizes the results of the Bayesian estimation for all three models when fitted with correct specifications. The posterior mean of each parameter was considered as the point estimator. The empirical bias of the estimates for all parameters is close to zero

Table 2: Model comparison result with DIC and LPML with sample size  $n \in \{200, 400, 800, \text{and}, 1600\}$ . Freq (%): frequency of the correct model being selected; Mean: average of the DIC or LPML.

True Model	Criterion	$n$	correlated-frailty		independent-frailty		shared-frailty	
			Freq	Mean	Freq	Mean	Freq	Mean
correlated-frailty	DIC	200	61	11889.5	23	11898.0	16	11900.9
		400	81	23812.5	14	23829.4	5	23844.9
		800	94	47324.2	4	47364.0	2	47394.8
		1600	95	94528.6	1	94612.9	4	94741.0
	LPML	200	50	-5957.2	27	-5960.7	23	-5961.7
		400	68	-11922.6	19	-11931.2	13	-11936.6
		800	87	-23682.2	7	-23702.5	6	-23715.7
		1600	90	-47292.0	4	-47332.0	6	-47395.2
independent-frailty	DIC	200	22	10885.3	71	10884.2	7	10901.7
		400	23	21701.9	75	21700.4	2	21747.0
		800	32	43296.2	68	43295.4	0	43391.4
		1600	28	86551.1	72	86549.6	0	86744.6
	LPML	200	19	-5448.0	72	-5446.6	9	-5457.0
		400	18	-10857.3	79	-10855.7	3	-10880.8
		800	25	-21655.6	74	-21653.6	1	-21703.5
		1600	19	-43284.7	81	-43282.6	0	-43381.7
shared-frailty	DIC	200	7	12415.9	0	12445.3	93	12405.9
		400	9	24773.1	0	24844.2	91	24758.6
		800	11	49302.4	0	49453.9	89	49282.7
		1600	23	98722.2	0	99038.5	77	98702.1
	LPML	200	11	-6221.9	2	-6238.7	87	-6214.7
		400	16	-12410.4	1	-12448.2	83	-12401.2
		800	22	-24680.6	1	-24760.0	77	-24671.1
		1600	30	-49397.1	0	-49556.2	70	-49386.0

except that of  $\theta_2$  when  $n = 200$  for the correlated-frailty and the independent-frailty model; in both cases the bias reduces as  $n$  increases. The mean of the posterior standard deviation of the estimates agrees closely with the empirical standard deviation of the point estimates for most parameters even for sample size  $n = 200$ . Consequently, the empirical coverage rates of the 95% highest posterior density (HPD) credible intervals are close to the nominal level, and the agreement improves in general as  $n$  increases from 200 to 400.

To evaluate the performance of model comparison criteria, we fitted three models to each dataset. DIC and LPML were used to select among the three fitted models. The Monte Carlo sample size used for approximating the integrals was set to be  $M = 500$ . Table 2 summarizes the frequencies under each criterion that the correct model was selected based on either DIC or LPML for sample size  $n \in \{200, 400, 800, \text{and}, 1600\}$ . On average, the correctly specified models have the smallest DIC and highest LPML. The results suggest good performance of both DIC and LPML in selecting the right models. For example, when correlated-frailty model is the data generating model, the proportion of correctly identify the true model increases for both DIC and LPML as the sample size increasing, which are 95% and 90%, respectively, with DIC slightly outperforming LPML. When the two reduced models are the data generating models, both DIC and LPML still select them with the highest frequency, but the tendency to choose the full model also increases when the sample size increases. Such observations echo the limitations of DIC and LPML in distinguishing the true model and an overfitted model (Maity et al., 2021). In our application, both criteria select either the correct model or the full model, which still provides valuable information for practitioners.

## 5 Hypoglycemic Event Time Analysis

The proposed model was applied to analyze the hypoglycemic event times from the DURABLE trial (Buse et al., 2009). Between 2005 and 2007, 2187 patients with type 2 diabetes from 11 countries were enrolled in the study. The dataset contains the possibly censored times of hypoglycemic events of the patients during their follow-up periods. Also, available are a collection of baseline covariates, which allows assessments of risk factors of hypoglycemia among the patients. The median follow-up time of the patients is 168 days. Continuous baseline covariates include fasting blood glucose, fasting insulin, adiponectin, weight, height, body mass index (BMI), systolic blood pressure, diastolic blood pressure, heart rate, and



Table 3: Summary of the covariates from the DURABLE trial. BMI, body mass index; BP, blood pressure; SD, standard deviation.

Variable	Minimum	Median	Maximum	Mean	SD
Fasting glucose (mmol/l)	0.23	10.45	25.96	10.78	3.72
Adiponectin ( $\mu\text{g}/\text{mL}$ )	0.01	5.57	49.01	6.99	5.52
Fasting insulin (mIU/L)	0.18	7.91	142.68	10.40	9.81
Height (cm)	124.25	166.44	198.09	166.47	10.71
BMI ( $\text{kg}/\text{m}^2$ )	15.88	31.28	62.62	31.71	6.18
Diastolic BP (mmHg)	45.01	78.70	116.30	78.23	9.46
Systolic BP (mmHg)	47.26	130.02	196.67	131.53	16.11
Heart rate (beats per minute)	43.86	76.61	121.05	76.76	9.82
Duration diabetes (years)	0.03	8.57	39.48	9.75	6.17

duration of diabetes. Summaries of the continuous covariates are presented in Table 3. Three important variables, fasting glucose level, adiponectin level, and fasting insulin level, have extremely high values, which calls for prudence in data analysis. Two categorical variables are available. The first one is starter insulin regimens with two levels, twice-daily lispro mix 75/25 (LM75/25; 75% lispro protamine suspension, 25% lispro) versus once-daily insulin glargine. The second one is the usage of oral antihyperglycemic drugs with three levels, thiazolidinedione, sulfonylurea, and both. All the available covariates are subject-level and time-independent covariates.

After excluding the subjects with missingness in covariates or outside reference range, the dataset contains  $n = 1943$  patients. Prior to model fitting, all the continuous covariates were standardized. Log transformation was applied to two right-skewed covariates, baseline adiponectin and baseline fasting insulin, before standardization. Among the 1943 patients, 570 (29%) received both oral antihyperglycemic drugs, 1207 (62%) only received sulfonylurea, and 166 (9%) only received thiazolidinedione. For ease of discussion, the group that received both of two drugs were used as the reference group; two dummy variables, **sulf-Only**, which is 1 if only received sulfonylurea, and **tzd-only**, which is 1 if only received thiazolidinedione, were included. Define an indicator variable for the insulin regime **LM**, which equals 1 for the

Table 4: Model comparison for three models (correlated-frailty, independent-frailty, and shared-frailty model) fitted to the DURABLE data.

	correlated-frailty	independent-frailty	shared-frailty
DIC	131400.8	131397.0	131944.6
LPML	-65707.5	-65706.7	-65986.7

959 (49%) patients who received LM 75/25 and 0 for the 984 (51%) patients who received glargine. Some patients had multiple hypoglycemic events within a single calendar date. In this case, the gap times between successive hypoglycemic events were recorded as zero. This is handled by treating the gap times in days as interval-censored with the likelihood constructed with (3.1) in Section 3.1. The daily hypoglycemic event rates of the patients have a wide range from 0 to 0.77 with mean 0.07. These descriptive statistics indicate the existence of severe heterogeneity risk of hypoglycemia among subjects.

The three models along with their priors investigated in Section 4 were fitted to the DURABLE data. The lower boundary was set to 3.9 mmol/l (70 mg/dl), which is the clinical standard for hypoglycemic events (Seaquist et al., 2013). The starting point  $x_0$  of the Brownian motion after each hypoglycemic event was set to be 10, which is the rounded integer of the mean of the baseline fasting glucose level of all the patients. The sensitivity analysis of different priors and starting points have been conducted and the results showed that the estimates of the covariate effects are stable, which can be found in the Supplementary Materials. For each model, an MCMC was run for 55,000 iterations and thinned by 10 after discarding the first 15,000 iterations as burn-in. The convergence of the MCMC chains was monitored by trace plots. The results of DIC and LPML for the three models are presented in Table 4. Both criteria suggest that the correlated-frailty model and the independent-frailty model are similar, both of which are preferred to shared-frailty model. Given that the correlated-frailty and the independent-frailty have close model fit, we chose the independent-frailty model as it is parsimonious. That is, the two frailties in the upper reflection barrier and the volatility could be treated as independent.

Table 5: Estimated parameters of the independent-frailty model. BMI, body mass index; BP, blood pressure; SD, standard deviation; CI, 95% HPD credible interval or 95% confident interval.

Covariates	Independent-frailty Model				Proportional hazards gap time			
	Volatility		Upper reflection barrier		Mean	SD	95% CI	95% CI
	Mean	SD	95% CI	Mean				
Intercept	0.910	0.036	<b>[0.840, 0.982]</b>	2.868	0.067	<b>[2.745, 2.999]</b>	-	-
Fasting glucose	-0.054	0.019	<b>[-0.096, -0.017]</b>	0.108	0.031	<b>[0.049, 0.170]</b>	-0.122	<b>[-0.169, -0.075]</b>
Adiponectin	0.046	0.019	<b>[0.011, 0.085]</b>	0.030	0.031	<b>[-0.035, 0.088]</b>	0.042	<b>[-0.008, 0.093]</b>
Fasting insulin	-0.107	0.022	<b>[-0.150, -0.065]</b>	0.169	0.032	<b>[0.108, 0.231]</b>	-0.208	<b>[-0.259, -0.157]</b>
Height	-0.047	0.019	<b>[-0.085, -0.011]</b>	0.004	0.032	<b>[-0.056, 0.068]</b>	-0.059	<b>[-0.107, -0.012]</b>
BMI	-0.089	0.021	<b>[-0.132, -0.046]</b>	-0.113	0.033	<b>[-0.180, -0.050]</b>	-0.058	<b>[-0.109, -0.006]</b>
Diastolic BP	-0.069	0.022	<b>[-0.110, -0.025]</b>	0.055	0.036	<b>[-0.018, 0.122]</b>	-0.109	<b>[-0.164, -0.053]</b>
Systolic BP	0.025	0.020	<b>[-0.012, 0.064]</b>	-0.027	0.032	<b>[-0.094, 0.033]</b>	0.041	<b>[-0.013, 0.094]</b>
Heart rate	0.008	0.018	<b>[-0.027, 0.042]</b>	0.048	0.029	<b>[-0.009, 0.104]</b>	-0.011	<b>[-0.058, 0.036]</b>
Duration diabetes	0.081	0.018	<b>[0.049, 0.117]</b>	-0.049	0.028	<b>[-0.105, 0.004]</b>	0.120	<b>[0.074, 0.166]</b>
LM	0.168	0.036	<b>[0.098, 0.240]</b>	-0.102	0.061	<b>[-0.219, 0.017]</b>	0.236	<b>[0.145, 0.326]</b>
tzd-only	-0.490	0.072	<b>[-0.628, -0.351]</b>	0.322	0.149	<b>[0.035, 0.614]</b>	-0.673	<b>[-0.868, -0.479]</b>
sulf-only	-0.022	0.037	<b>[-0.093, 0.054]</b>	0.059	0.066	<b>[-0.067, 0.195]</b>	-0.064	<b>[-0.175, 0.047]</b>
Frailty Variance	0.408	0.026	<b>[0.356, 0.458]</b>	0.535	0.044	<b>[0.450, 0.620]</b>	0.759	-

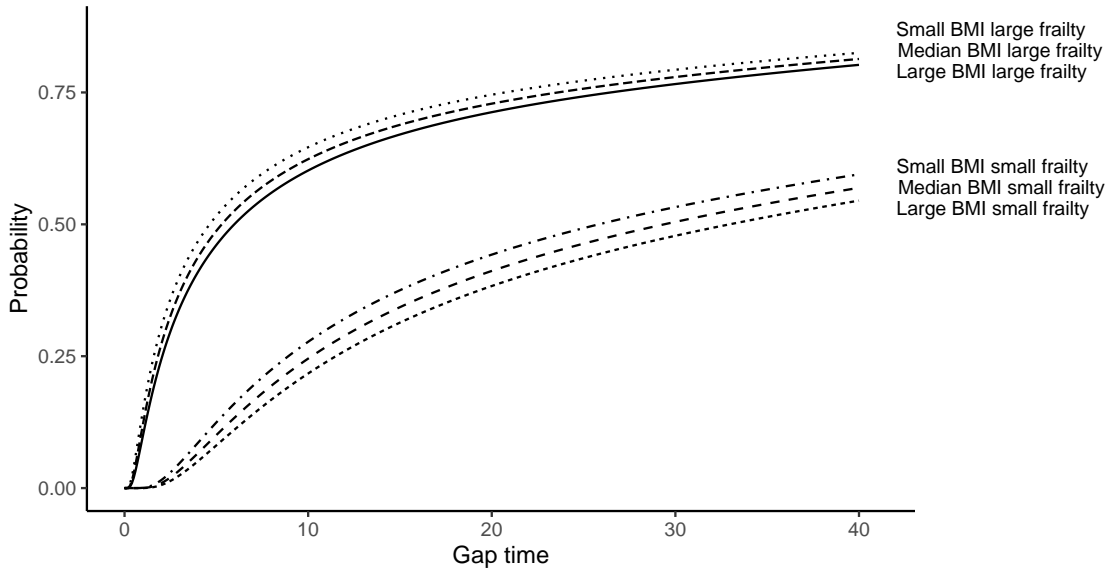


Figure 2: First hitting time distribution with fitted parameters of independent-frailty model. Distribution functions are derived from 6 combinations of 3 levels of BMI, small, median, and large, which represent the 25%, 50%, and 75% quantile of the standardized BMI, respectively; and 2 levels of frailties, small and large, which represent the 25% and 75% quantile of the frailty distributions both in volatility  $\sigma$  and upper reflection barrier  $\kappa$ . Other covariates remain the same at their median level after being standardized.

Table 5 summarizes the estimated model parameters, their standard errors, and 95% HPD credible confidence intervals from the fitted independent-frailty model. The results from the volatility model suggest that patients with higher baseline fasting blood glucose level, lower adiponectin, higher fasting insulin, higher height, higher BMI, higher diastolic BP, lower duration of diabetes are significantly associated with lower volatility and, hence, lower risk of hypoglycemia. Patients who received LM 75/25 appear to have higher volatility or higher risk of hypoglycemia compared to those who received glargine. For the oral antihyperglycemic drugs, patients who received only thiazolidinedione appear to have lower volatility or lower risk of hypoglycemia compared to those who received both thiazolidinedione and sulfonylurea; patients who received only sulfonylurea are not significantly different from those who received both.

In the upper reflection barrier model, fewer covariates are significant and they are a subset of those that are significant in the volatility model. Patients with higher baseline

fasting blood glucose level, higher fasting insulin, and lower BMI are associated higher reflection barrier and, hence, lower risk of hypoglycemia. For the oral antihyperglycemic drugs, patients who received only thiazolidinedione appear to have higher reflection barrier and, hence, lower risk of hypoglycemia compared to those who received both thiazolidinedione and sulfonylurea. Interestingly, the effect of baseline fasting blood glucose level, fasting insulin, and received only thiazolidinedione, the coefficients have the same direction on the risk of hypoglycemia in the models for volatility and upper reflection barrier (with opposite coefficient signs). In contrast, BMI is significant in affecting both the volatility and the upper reflecting barrier, but with opposite directions (with the same coefficient signs). That is, the overall effect of BMI on the risk of hypoglycemia is complicated by lowering the volatility (or lowering the risk) while decreasing the upper reflection barrier (or increasing the risk). This discovery has not been reported in the quantile regression analysis of [Ma et al. \(2021\)](#). But the overall effects of baseline BMI is worth further investigating. Figure 2 gives a set of the first hitting time distributions with the fitted parameters of independent-frailty model using different levels of baseline BMI and frailties. From Figure 2, regardless of the frailty level, smaller BMI is associated with a higher risk of having hypoglycemic events.

Comparison of the estimates between the proposed model and proportional hazards model of gap time between recurrent events is also given in Table 5. With the exception of the covariate Adiponectin, the other covariates exhibit similar levels of significance between proportional hazards model and volatility in the proposed model. For Adiponectin, the estimates in the volatility and upper reflection barrier model are  $0.046[0.011, 0.085]$  and  $0.030[-0.035, 0.088]$ , respectively, in the proposed model. This suggests that Adiponectin contributes in different directions on volatility and upper reflection barrier model for the recurrent risk. Given that the volatility component exerts a stronger influence on recurrence, our estimate indicates that the higher value of Adiponectin is associated with an increased risk of recurrence. In proportional hazards model, the estimate of Adiponectin is  $0.042[-0.008, 0.093]$ , aligning with the trend observed in the proposed model. For the

other significant covariates, the signs of estimates between the volatility model and proportional hazards model are consistent. This observation suggests that, for this dataset, the proposed model offers a more detailed characterization of the concealed glucose levels linked to recurrent events.

The two independent frailties in the volatility and the upper reflection barrier capture much of the heterogeneity among the patients beyond the covariates. The variances of the two frailties are estimated to be far away from zero. From the fitted model, the range of volatility spans from 0.65 to 9.52 with median 2.75 and mean 3.03; the range of upper reflection barrier spans from 12.69 to 83.47 with median 29.57 and mean 29.88. The model without the frailties fits much poorer in terms of DIC and LPML (not reported).

## 6 Discussion

The risk of hypoglycemia is an important concern in diabetes management. It is natural to model the underlying blood glucose level as hypoglycemia occurs when it hits a lower boundary and hyperglycemia occurs when it hits an upper boundary. Because of the unique setting where hyperglycemia cannot be reliably observed in self-reported data, it is challenging to model the blood glucose level as a stochastic process. The proposed Brownian motion model with an upper reflection barrier allows bypassing the need for observing hyperglycemic event times. Only hypoglycemic times are needed for the model fitting. This model fitting is made possible by the FHT density and distribution (Hu et al., 2012). The recurrence of the hypoglycemic events is captured by a sequence of stochastic processes reaching the lower-boundary. The upper reflection barrier and volatility of the reflected Brownian motion are linked to patient-level covariates and frailties. Due to the unobserved frailties, we resorted to Bayesian inference for the parameters with MCMC implemented with NIMBLE (de Valpine et al., 2017). The computation of our work relies on an accurate implementation of the FHT density/distribution functions as well as the rejection sampling algorithm with the 3-piece

proposal kernel. Another computation challenge is the complexity brought by unobserved frailties in calculating model selection criteria DIC and LPML. We applied Monte Carlo integration for an approximation, with which the two criteria were shown to be reasonably effective in selecting the correct frailty model by simulation studies.

It is worthwhile to revisit the key model assumptions. In our model, the imposed upper reflection barrier reflects the expectation that the blood sugar level is bounded and will not reach infinity. This modeling choice aids in illustrating that glucose levels will ultimately be controlled (dropping down) in the range. We believe this assumption is reasonable, especially for participants who are consistently under regular blood sugar maintenance. Another key assumption is that the glucose level returns to normal immediately following the occurrence of the hypoglycemia event. In reality, it certainly takes time to consume food and bring back the glucose level, but the recovery is usually in minutes and, thus, quick enough so we neglect the time used. We also assumed that, after a hypoglycemia event, the glucose level restarts at a fixed level  $x_0$ . A sensitivity analysis with different values of  $x_0$  showed little difference in the resulting regression coefficient estimates.

Under the model framework, a subject with larger volatility and lower upper reflection barrier is associated with higher risk of the hypoglycemia event. In our experience, the covariate with the same direction on the risk of hypoglycemia (with opposite coefficient signs in volatility and upper reflection barrier) is usually consistent with that of the classic gap time models. On the other hand, if a covariate contributes a positive (negative) effect to both the volatility and upper reflection barrier, its overall impact is less straightforward. In this case, it is possible that the covariate shows no significant impact from the classic gap time models, while play an import role for volatility or upper reflection barrier. An example of this is the covariate Adiponectin in our data application. Therefore, despite its complexity, the proposed model provides additional insights for a better understanding of the data. To further investigate the covariate overall effect of proposed model, we recommend plotting the FHT distribution to provide an overall characterization of the impact of this covariate.

Several directions are worth further investigation. In the broad sense, the proposed model can be applied to scenarios where an event occurs when an underlying health level process hits a boundary on one side. Therefore, many of the examples based on Wiener process reviewed in [Lee and Whitmore \(2006\)](#) are potentially applicable. The Wiener process approach ensures finiteness of the FHT by a nonzero drift. Our process does so with a reflecting boundary on the other side for a driftless Wiener process. When the reflecting boundary is removed, the FHT has a positive probability of being infinity, which makes it applicable when a cure rate is needed ([Lee and Whitmore, 2006](#), Section 5). Finally, the DURABLE dataset has additional longitudinally observed blood glucose levels. To combine these longitudinal observations with the hypoglycemic events into a joint modeling framework, the transition density of a reflected Brownian motion would be needed. Incorporating this density into our framework would be interesting but not trivial.

## Supplementary Materials

Supplementary Materials include (A) sensitivity analyses for the application with different priors and (B) different choices of starting point  $x_0$ , (C) trace plots for the parameters in independent-frailty model of two MCMC chains, and (D) code examples.

### A Tail of FHT Density

Here we show that the right tail of the FHT is bounded by an exponential rate. Note that rates  $\lambda_n$  monotonically increase to  $\infty$  as  $n \rightarrow \infty$  (so,  $\lambda_1$  is the slowest rate),  $c_1 > 0$ , and  $|c_n| < 1$  for  $n \geq 2$ . It can be shown that density  $f(t)$  is asymptotically equivalent to  $c_1 \lambda_1 e^{-\lambda_1 t}$  as  $t \rightarrow \infty$ .



First, let us rewrite the FHT density as follows:

$$f(t) = \sum_{n=1}^{\infty} c_n \lambda_n e^{-\lambda_n t} = c_1 \lambda_1 e^{-\lambda_1 t} \left( 1 + \frac{1}{c_1 \lambda_1} \sum_{n=2}^{\infty} c_n \lambda_n e^{-(\lambda_n - \lambda_1)t} \right),$$

where  $\lambda_n = b(2n - 1)^2$  and  $b = \frac{\sigma^2 \pi^2}{8(\kappa - \nu)^2}$ .

Now, consider  $h(t) = \sum_{n=2}^{\infty} c_n \lambda_n e^{-(\lambda_n - \lambda_1)t}$  and observe that

$$\begin{aligned} |h(t)| &= \left| \sum_{n=2}^{\infty} c_n \lambda_n e^{-(\lambda_n - \lambda_1)t} \right| = e^{-bt} \left| \sum_{n=2}^{\infty} c_n \lambda_n e^{-(\lambda_n - \lambda_1 - b)t} \right| \\ &\leq e^{-bt} \sum_{n=2}^{\infty} |c_n| \lambda_n e^{-(\lambda_n - \lambda_1 - b)t} \leq e^{-bt} \sum_{n=2}^{\infty} \lambda_n e^{-(\lambda_n - \lambda_1 - b)t}. \end{aligned}$$

Therefore, if  $\sum_{n=2}^{\infty} \lambda_n e^{-(\lambda_n - \lambda_1 - b)t}$  is bounded for all sufficiently large  $t$ , then  $|h(t)| \rightarrow 0$  as  $t \rightarrow \infty$ . Indeed, since  $\lambda_n - \lambda_1 - b = b(2n - 1)^2 - 2b > 0$  for  $n \geq 2$ , for  $t > 1$  we have

$$\sum_{n=2}^{\infty} \lambda_n e^{-(\lambda_n - \lambda_1 - b)t} \leq \sum_{n=2}^{\infty} \lambda_n e^{-(\lambda_n - \lambda_1 - b)*1} = e^{\lambda_1 + b} \sum_{n=2}^{\infty} \lambda_n e^{-\lambda_n} < \infty,$$

because  $\sum_{n=2}^{\infty} \lambda_n e^{-\lambda_n}$  is obviously a convergent series. Thus, hitting time density  $f(t) \sim c_1 \lambda_1 e^{-\lambda_1 t}$  as  $t \rightarrow \infty$ .

This result allows the use of an exponential distribution, with proper scaling, on the right tail to bound the FHT density as detailed next.

## B Rejection Sampling Algorithm

To sample from the FHT density  $f$ , we handle the left tail, body, and right tail separately. Define  $g_1(t)$ ,  $g_2(t)$ , and  $g_3(t)$  as the proposal density for the left, body, and right components, respectively,

$$g_1(t) \propto k_1 t, \quad t \leq t_m,$$

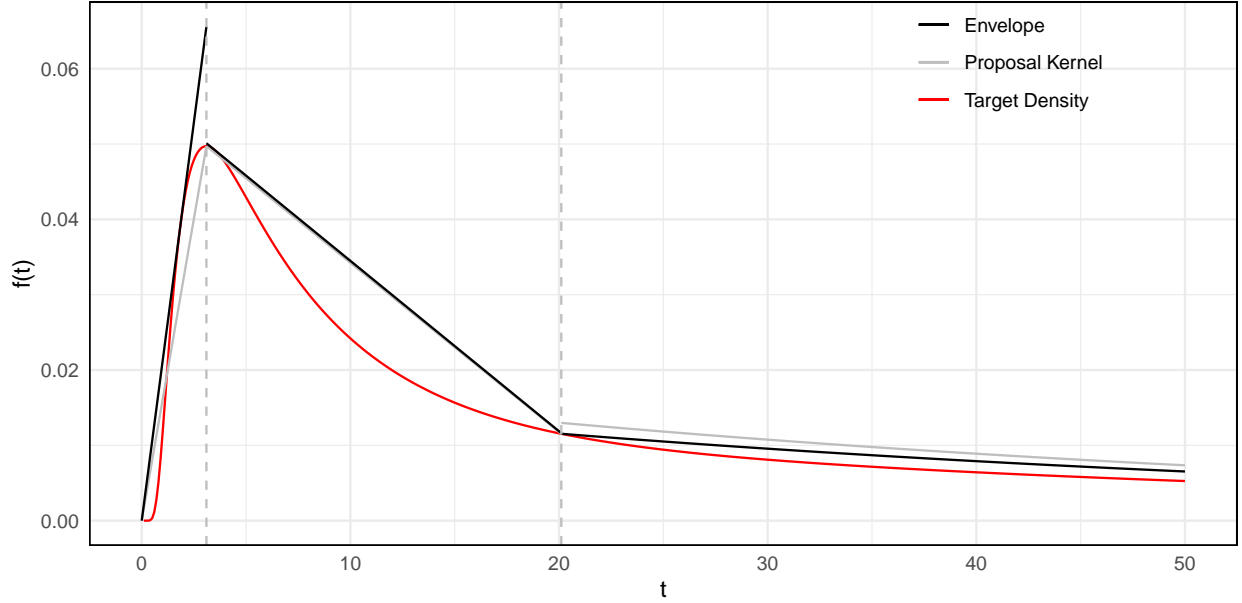


Figure 3: Actual density of the first hitting time distribution of the reflected Brownian motion with  $x_0 = 10$ ,  $\kappa = 20$ ,  $\nu = 3.9$ ,  $\sigma = 2$  is given as red line. The three-piece kernel and the envelope resulting from the multiplication of corresponding constants with the kernel are given grey line and black line respectively. In this plot,  $q = 0.5$  is considered

$$\begin{aligned}
 g_2(t) &\propto k_2 t + f(t_m) - k_2 t_m, & t_m < t \leq t_q, \\
 g_3(t) &\propto \exp(-\lambda_1 t), & t > t_q,
 \end{aligned}$$

where  $k_1 = f(t_m)/t_m$  and  $k_2 = [f(t_m) - f(t_q)]/(t_m - t_q)$ . For illustration, Figure 3 shows the actual (target) density of first hitting distribution in red, the kernels of the three proposal densities in grey, and the envelopes derived by multiplying corresponding constants to the kernels in black. Given the shape properties of  $f$ , the  $i$ th component of  $f$  can be bounded by  $M_i g_i(t)$ , where  $M_i$  can be identified by maximizing  $f(t)/g_i(t)$  over the domain of  $g_i$ ,  $i = 1, 2, 3$ .

The rejection sampling algorithm for generating one observation from  $f$  is given in Algorithm 1.

---

**Algorithm 1:** Rejection sampling algorithm for drawing one observation from the FHT density.

---

**Algorithm:**

**Input:**  $f$  and  $F$ , the FHT density and distribution functions;  
 $q$ , a user defined percentile;  
 $q_{t_m} = F(t_m)$ ;  
 $g_1, g_2$ , and  $g_3$ , three component proposals;  
 $M_1, M_2$ , and  $M_3$ , bounding constants for the three components;

**Output:**  $Y$ , a draw from target density  $f$

Draw  $U \sim \text{Uniform}(0, 1)$

**if**  $U \leq q_{t_m}$  **then**

**repeat**

        Draw candidate  $Y \sim g_1$

        Draw  $U' \sim \text{Uniform}(0, 1)$

**until**  $U' \leq f(Y)/[M_1 g_1(Y)]$

**else if**  $q_{t_m} < U \leq q$  **then**

**repeat**

        Draw candidate  $Y \sim g_2$

        Draw  $U' \sim \text{Uniform}(0, 1)$

**until**  $U' \leq f(Y)/[M_2 g_2(Y)]$

**else if**  $U > q$  **then**

**repeat**

        Draw candidate  $Y \sim g_3$

        Draw  $U' \sim \text{Uniform}(0, 1)$

**until**  $U' \leq f(Y)/[M_3 g_3(Y)]$

**return**  $Y$

---

## References

Andersen, P. K. and R. D. Gill (1982). Cox's regression model for counting processes: A large sample study. *The Annals of Statistics* 10(4), 1100–1120.

Box-Steffensmeier, J. M. and S. De Boef (2006). Repeated events survival models: The conditional frailty model. *Statistics in Medicine* 25(20), 3518–3533.

Buse, J. B., B. H. Wolffenbuttel, W. H. Herman, N. K. Shemonsky, H. H. Jiang, J. L. Fahrback, J. L. Scism-Bacon, and S. A. Martin (2009). Durability of basal versus lispro mix 75/25 insulin efficacy (Durable) trial 24-week results: Safety and efficacy of insulin

- lispro mix 75/25 versus insulin glargine added to oral antihyperglycemic drugs in patients with type 2 diabetes. *Diabetes Care* 32(6), 1007–1013.
- Celeux, G., F. Forbes, C. P. Robert, and D. M. Titterington (2006). Deviance information criteria for missing data models. *Bayesian Analysis* 1(4), 651–673.
- Centers for Disease Control and Prevention (2022). National diabetes statistics report website. Accessed Oct 28, 2022.
- Chang, S.-H. (2004). Estimating marginal effects in accelerated failure time models for serial sojourn times among repeated events. *Lifetime Data Analysis* 10(2), 175–190.
- Charles-Nelson, A., S. Katsahian, and C. Schramm (2019). How to analyze and interpret recurrent events data in the presence of a terminal event: An application on readmission after colorectal cancer surgery. *Statistics in Medicine* 38(18), 3476–3502.
- Cook, R. J. and J. F. Lawless (2007). *The Statistical Analysis of Recurrent Events*. New York: Springer.
- Cryer, P. E., L. Axelrod, A. B. Grossman, S. R. Heller, V. M. Montori, E. R. Seaquist, and F. J. Service (2009). Evaluation and management of adult hypoglycemic disorders: An Endocrine Society Clinical Practice Guideline. *The Journal of Clinical Endocrinology and Metabolism* 94(3), 709–728.
- Cryer, P. E., S. N. Davis, and H. Shamoan (2003). Hypoglycemia in diabetes. *Diabetes Care* 26(6), 1902–1912.
- de Valpine, P., D. Turek, C. Paciorek, C. Anderson-Bergman, D. Temple Lang, and R. Bodik (2017). Programming with models: Writing statistical algorithms for general model structures with NIMBLE. *Journal of Computational and Graphical Statistics* 26, 403–413.
- DeRosa, M. A. and P. E. Cryer (2004). Hypoglycemia and the sympathoadrenal system: Neurogenic symptoms are largely the result of sympathetic neural, rather

- than adrenomedullary, activation. *American Journal of Physiology-Endocrinology and Metabolism* 287(1), E32–E41.
- Dey, D. K., M.-H. Chen, and H. Chang (1997). Bayesian approach for nonlinear random effects models. *Biometrics* 53(4), 1239–1252.
- Doubleday, K., J. Zhou, H. Zhou, and H. Fu (2022). Risk controlled decision trees and random forests for precision medicine. *Statistics in Medicine* 41(4), 719–735.
- Duchateau, L., P. Janssen, I. Kezic, and C. Fortpied (2003). Evolution of recurrent asthma event rate over time in frailty models. *Journal of the Royal Statistical Society Series C: Applied Statistics* 52(3), 355–363.
- Economou, P., S. Malefaki, and C. Caroni (2015). Bayesian threshold regression model with random effects for recurrent events. *Methodology and Computing in Applied Probability* 17(4), 871–898.
- Folks, J. L. and R. S. Chhikara (1978). The inverse gaussian distribution and its statistical application — A review. *Journal of the Royal Statistical Society: Series B (Methodological)* 40(3), 263–275.
- Fu, H., J. Luo, and Y. Qu (2016). Hypoglycemic events analysis via recurrent time-to-event (Heart) models. *Journal of Biopharmaceutical Statistics* 26(2), 280–298.
- Geisser, S. and W. F. Eddy (1979). A predictive approach to model selection. *Journal of the American Statistical Association* 74(365), 153–160.
- Gelfand, A. E. and D. K. Dey (1994). Bayesian model choice: Asymptotics and exact calculations. *Journal of the Royal Statistical Society: Series B (Methodological)* 56(3), 501–514.
- Gelman, A. (2006). Prior distributions for variance parameters in hierarchical models (comment on article by Browne and Draper). *Bayesian Analysis* 1(3), 515–534.

- Heidelberger, P. and P. D. Welch (1983). Simulation run length control in the presence of an initial transient. *Operations Research* 31(6), 1109–1144.
- Hofert, M., I. Kojadinovic, M. Mächler, and J. Yan (2018). *Elements of Copula Modeling with R*. Springer.
- Hu, Q., Y. Wang, and X. Yang (2012). The hitting time density for a reflected brownian motion. *Computational Economics* 40(1), 1–18.
- Huang, Y. and Y. Q. Chen (2003). Marginal regression of gaps between recurrent events. *Lifetime Data Analysis* 9, 293–303.
- Klein, J. P. (1992). Semiparametric estimation of random effects using the Cox model based on the EM algorithm. *Biometrics* 48(3), 795–806.
- Lawless, J. F. and C. Nadeau (1995). Some simple robust methods for the analysis of recurrent events. *Technometrics* 37(2), 158–168.
- Lee, E. W., L. Wei, D. A. Amato, and S. Leurgans (1992). Cox-type regression analysis for large numbers of small groups of correlated failure time observations. In J. P. Klein and P. K. Goel (Eds.), *Survival Analysis: State of the Art*, pp. 237–247. Springer.
- Lee, M.-L. T. (2019). A survey of threshold regression for time-to-event analysis and applications. *Taiwanese Journal of Mathematics* 23(2), 293–305.
- Lee, M.-L. T. and G. A. Whitmore (2006). Threshold regression for survival analysis: Modeling event times by a stochastic process reaching a boundary. *Statistical Science* 21(4), 501–513.
- Lin, D. Y., L.-J. Wei, I. Yang, and Z. Ying (2000). Semiparametric regression for the mean and rate functions of recurrent events. *Journal of the Royal Statistical Society: Series B (Statistical Methodology)* 62(4), 711–730.

- Luo, X., C.-Y. Huang, and L. Wang (2013). Quantile regression for recurrent gap time data. *Biometrics* 69(2), 375–385.
- Ma, H., L. Peng, C.-Y. Huang, and H. Fu (2021). Heterogeneous individual risk modelling of recurrent events. *Biometrika* 108(1), 183–198.
- Maity, A. K., S. Basu, and S. Ghosh (2021). Bayesian criterion-based variable selection. *Journal of the Royal Statistical Society Series C: Applied Statistics* 70(4), 835–857.
- Malefaki, S., P. Economou, and C. Caroni (2015). Modelling times between events with a cured fraction using a first hitting time regression model with individual random effects. In C. P. Kitsos, T. A. Oliveira, A. Rigas, and S. Gulati (Eds.), *Theory and Practice of Risk Assessment*, pp. 45–65. Springer.
- Manda, S. O. and R. Meyer (2005). Bayesian inference for recurrent events data using time-dependent frailty. *Statistics in Medicine* 24(8), 1263–1274.
- Pennell, M. L., G. Whitmore, and M.-L. Ting Lee (2010). Bayesian random-effects threshold regression with application to survival data with nonproportional hazards. *Biostatistics* 11(1), 111–126.
- Plummer, M., N. Best, K. Cowles, and K. Vines (2006). CODA: Convergence diagnosis and output analysis for MCMC. *R News* 6(1), 7–11.
- Prentice, R. L., B. J. Williams, and A. V. Peterson (1981). On the regression analysis of multivariate failure time data. *Biometrika* 68(2), 373–379.
- Schaubel, D. E. and J. Cai (2004). Regression methods for gap time hazard functions of sequentially ordered multivariate failure time data. *Biometrika* 91(2), 291–303.
- Schrödinger, E. (1915). Zur theorie der fall-und steigversuche an teilchen mit brownscher bewegung. *Physikalische Zeitschrift* 16, 289–295.

- Seaquist, E. R., J. Anderson, B. Childs, P. Cryer, S. Dagogo-Jack, L. Fish, S. R. Heller, H. Rodriguez, J. Rosenzweig, and R. Vigersky (2013). Hypoglycemia and diabetes: A report of a workgroup of the American Diabetes Association and the Endocrine Society. *Diabetes Care* 36(5), 1384–1395.
- Spiegelhalter, D. J., N. G. Best, B. P. Carlin, and A. Van Der Linde (2002). Bayesian measures of model complexity and fit. *Journal of the Royal Statistical Society: Series B (Statistical Methodology)* 64(4), 583–639.
- Sun, L., D.-H. Park, and J. Sun (2006). The additive hazards model for recurrent gap times. *Statistica Sinica* 16(3), 919–932.
- Towler, D. A., C. E. Havlin, S. Craft, and P. Cryer (1993). Mechanism of awareness of hypoglycemia: Perception of neurogenic (predominantly cholinergic) rather than neuroglycopenic symptoms. *Diabetes* 42(12), 1791–1798.
- Wei, L.-J., D. Y. Lin, and L. Weissfeld (1989). Regression analysis of multivariate incomplete failure time data by modeling marginal distributions. *Journal of the American Statistical Association* 84(408), 1065–1073.
- Whitmore, G., T. Ramsay, and S. Aaron (2012). Recurrent first hitting times in Wiener diffusion under several observation schemes. *Lifetime Data Analysis* 18(2), 157–176.
- Wild, D., R. von Maltzahn, E. Brohan, T. Christensen, P. Clauson, and L. Gonder-Frederick (2007). A critical review of the literature on fear of hypoglycemia in diabetes: Implications for diabetes management and patient education. *Patient Education and Counseling* 68(1), 10–15.
- Xu, G., S. H. Chiou, J. Yan, K. Marr, and C.-Y. Huang (2020). Generalized scale-change models for recurrent event processes under informative censoring. *Statistica Sinica* 30, 1773.